

NOTICE CONCERNING COPYRIGHT RESTRICTIONS

This document may contain copyrighted materials. These materials have been made available for use in research, teaching, and private study, but may not be used for any commercial purpose. Users may not otherwise copy, reproduce, retransmit, distribute, publish, commercially exploit or otherwise transfer any material.

The copyright law of the United States (Title 17, United States Code) governs the making of photocopies or other reproductions of copyrighted material.

Under certain conditions specified in the law, libraries and archives are authorized to furnish a photocopy or other reproduction. One of these specific conditions is that the photocopy or reproduction is not to be "used for any purpose other than private study, scholarship, or research." If a user makes a request for, or later uses, a photocopy or reproduction for purposes in excess of "fair use," that user may be liable for copyright infringement.

This institution reserves the right to refuse to accept a copying order if, in its judgment, fulfillment of the order would involve violation of copyright law.

Analytical Solutions of Tracer Transport in Fractured Rock Associated with Precipitation-Dissolution Reactions

Hui-Hai Liu, Sumit Mukhopadhyay, Nicolas Spycher, and Burton M. Kennedy

Earth Sciences Division, Lawrence Berkeley National Laboratory,
University of California, Berkeley CA

Keywords

Tracer transport, EGS, analytical solution, fractured rock, fracture-matrix interaction, isotopic tracers

ABSTRACT

To provide a sustainable heat extraction rate, an Enhanced Geothermal System (EGS) requires adequate circulation of the working fluid through a heat exchanger, which is comprised of a network of open fractures. The permeability of the fracture network constrains the fluid flux, and the surface area of the matrix rocks in contact with the fluid constrains the power or efficiency of the heat exchanger. Consequently, these parameters (surface area and permeability) are crucial for determining the capacity and longevity of EGS systems. One promising approach to estimate these properties is to analyze natural and/or artificial tracer data that are subject to fracture-matrix interactions including matrix diffusion and a number of chemical reactions within the matrix. Analytical solutions for tracer transport are commonly used to analyze tracer test data. However, precipitation-dissolution reactions can impact the tracer behavior, and analytical solutions for tracer transport associated with precipitation-dissolution reactions are limited in the literature. This study develops analytical solutions for tracer transport in both a single-fracture and a multiple-fracture system associated with precipitation-dissolution reactions under transient and steady state transport conditions. These solutions also take into account advective transport in fractures and molecular diffusion in rock matrix. It is demonstrated that for studying distributions of disturbed tracer concentration (defined as difference between actual concentration and its equilibrium value), effects of precipitation-dissolution reactions are mathematically equivalent to a “decay” process with a decay constant proportional to the corresponding bulk reaction rate. This important feature significantly simplifies our derivation procedure by taking advantage of the existence of analytical solutions to tracer transport associated with radioactive decay in fractured rock. It is also useful for interpreting tracer breakthrough curves, because impact of

decay process is relatively easy to analyze. Several illustrative examples (breakthrough curves obtained from analytical solutions) are presented and show that results are quite sensitive to fracture spacing, fracture surface area, and bulk reaction rate (or “decay” constant), indicating that the relevant flow and transport parameters can be inferred by analyzing tracer signals.

1. Introduction

Tracer transport in fractured rock involves fast and advection-dominated processes in fractures characterized by high permeability and mass transfer between fractures and rock matrix in which chemical reactions may occur as well. Modeling tracer transport in fractured rock is of interest to a number of practical applications, including interpretation of isotopic tracer transport signals for characterizing flow patterns and fracture-matrix interactions in geothermal systems (e.g., DePaolo, 2006).

Practical applications of a variety of analytical solutions for tracer transport in fractured rock to field-scale problems have been widely documented in the literature (e.g., Neretnieks, 2002; DePaolo, 2006; Maloszewski and Zuber, 1985). Water flow in a saturated fractured rock is commonly characterized by one or several dominant flow paths. In these applications, tracer transport through one of the flow paths is approximated by the corresponding analytical solutions. A practical application is related to enhanced geothermal system (EGS) in which heat is mined using injection and production wells (MIT, 2007). An EGS corresponds to a geothermal reservoir (at a depth with high temperature) that is fractured artificially (Figure 1). A key parameter for an EGS is fracture-matrix interfacial area between injection and production wells, because the area is directly related to heat transfer from surrounding rock to working fluid (water) and therefore determines capacity and longevity of a geothermal power plant. Use of analytical solutions to analyze signals of natural and/or artificial tracers provide a promising and practical way to determine the area, because tracer transport is considerably impacted by the area through matrix diffusion and precipitation-dissolution reactions occurring in the rock matrix. The focus of this study is the development of relevant analytical solutions.

Previous analytical solutions for tracer transport in fractured rock consider chemical reactions such as radioactive decay and adsorption (represented by a retardation factor). To the best of our knowledge, the recent work of DePaolo (2006) probably represents the first effort to develop systematic analytical solutions to tracer transport in fractured rock associated with precipitation-dissolution reactions. That work was particularly focused on describing isotopic tracer transport. Developed relationships between isotopic signals and flow path properties were demonstrated to be useful for characterizing the corresponding fracture-matrix properties (DePaolo, 2006). However, the analytical solutions of DePaolo (2006) are limited to steady-state transport conditions. Transient solutions are required for describing isotopic tracer transport in more general cases. In this paper, we derive analytical solutions to tracer transport in fractured rock associated with precipitation-dissolution reactions under both steady-state and transient transport conditions. The derivation is based on the analytical inversions of Laplace transformation that are similar to those used by Tang et al. (1981) and Sudicky and Frind (1982). The usefulness of our solutions in describing tracer transport is also demonstrated under a number of conditions.

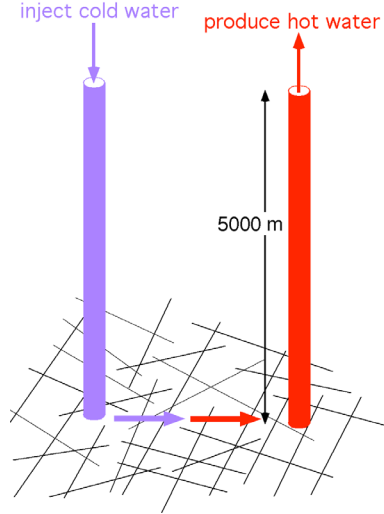


Figure 1. A sketch of enhanced geothermal system (EGS).

2. Assumptions and Governing Equations

We will investigate tracer transport in a single fracture or a set of equally spaced identical fractures. Note that focus herein is on solutions to tracer transport in fractures, rather than in matrix, although impact of rock matrix is exactly considered. This is simply because tracer concentration data are often obtained from fractures in practical applications (Neretnieks, 2002; DePaolo, 2006). Figure 2 shows a multiple-fracture system, with a single-fracture system being considered a special case with infinite fracture spacing. Water flow rate in each fracture is assumed to be constant and downward. Each fracture has a constant aperture that is much smaller than the fracture spacing. Matrix block has homogeneous properties and negligible permeability. Therefore, advection in rock matrix can be ignored. Because of transverse diffusion and dispersion, complete mixing across its width at all times. In other words, the solute concentration in the fracture is uniform across the fracture aperture. We also assume that molecular diffusion process within matrix occurs along the direction perpendicular to fractures only. The same assumptions were made in previous studies (e.g., Sudicky and Frind, 1982; DePaolo, 2006). Furthermore, we ignore the longitudinal dispersion and molecular diffusion within a fracture, because solute transport is advection dominated in a fracture and these processes (dispersion and dif-

fusion along the flow direction) are not important for practical applications (e.g., Neretnieks, 2002). Ignoring these processes can significantly simplify mathematical development of analytical solutions. Following DePaolo (2006), we also consider dissolution reaction rate to be the same as precipitation reaction rate within rock matrix. The justification for this treatment was provided in DePaolo (2006) within the context of isotopic tracer transport.

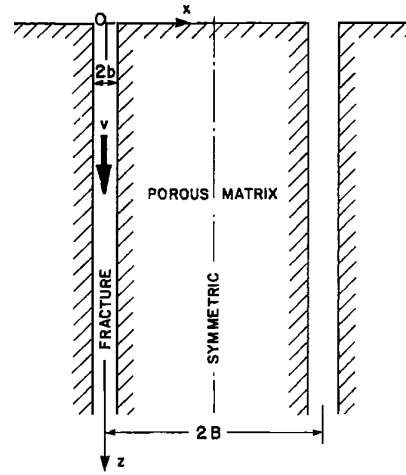


Figure 2. Fracture-matrix system.

With the above assumptions, tracer transport process in fractured rock can be described by two coupled equations for transport in liquid phase (one for fracture and one for rock matrix) and the third equation for solid phase due to precipitation-dissolution reactions. While the detailed derivation of these equations was given in DePaolo (2006), these equations are briefly discussed herein.

Based on the mass conservation principle, tracer transport in fractures is described by (Sudicky and Frind, 1982; DePaolo, 2006):

$$\frac{\partial c_f}{\partial t} = -v \frac{\partial c_f}{\partial z} + \frac{D_m \phi_m}{b} \left\langle \frac{\partial c_p}{\partial x} \right\rangle_{x=b} \quad (1)$$

where t is the time (T), z and x are the spatial coordinates (M) (Figure 2), c_f is the tracer concentration in fractures (M/L^3), v is the groundwater velocity in fractures (L/T), D_m is matrix diffusion coefficient defined by molecular diffusion coefficient in free water multiplied by tortuosity (L^2/T), ϕ_m is matrix porosity, c_p is the tracer concentration in matrix pore liquid (M/L^3), and $2b$ is the fracture aperture (L). The second term on the right hand of the equation describes the flux crossing two fracture walls.

Within the rock matrix, the pore fluid interacts with the solid phase by dissolution-precipitation, and the pore fluid communicates with the fracture fluid by diffusion. The equations describing these processes are given as (DePaolo, 2006):

$$\frac{\partial c_p}{\partial t} = D_m \frac{\partial^2 c_p}{\partial x^2} + R_m M (c_s - K_d c_p) \quad (2)$$

$$\frac{\partial c_s}{\partial t} = -R_m (c_s - K_d c_p) \quad (3)$$

where c_s is the tracer concentration in solid phase (M/L^3), R_m is the bulk (dissolution and precipitation) reaction rate (1/T) that was also called bulk reaction time constant by DePaolo (2006), K_d is the distribution coefficient for solid/fluid system, and M is the mass ratio of solid to liquid given by

$$M = \frac{\rho_s (1 - \phi_m)}{\rho_f \phi_m} \quad (4)$$

In Equation (4), ρ_f and ρ_s are fluid and solid density (M/L³). In Equation (2), terms $R_m Mc_s$ and $R_m MK_d c_p$ correspond to dissolution and precipitation, respectively. When these two terms are equal, dissolution and precipitation are in equilibrium.

For isotopic tracer transport processes with typical R_m values, DePaolo (2006) demonstrated that solid phase concentration c_s hardly changes because of low tracer concentration in the liquid phase in natural fracture rocks. Therefore, he assumed c_s to be constant during developing steady-state solutions for tracer transport. In this study, we follow the similar treatment and therefore need to solve Equations (1) and (2) only (as a result of assuming c_s to be a constant) for modeling tracer transport in liquid phase.

For convenience, we introduce the following variables:

$$C_p = c_p - \frac{c_s}{K_d} \quad (5-1)$$

$$C_f = c_f - \frac{c_s}{K_d} \quad (5-2)$$

$$\lambda = R_m MK_d \quad (5-3)$$

Note that under equilibrium conditions, $C_f = C_p = 0$; C_f and C_p can be considered as concentration disturbances to equilibrium concentration fields, because they represent differences between tracer concentrations and their equilibrium values. Combining Equations (1), (2) and (5) yields

$$\frac{\partial C_f}{\partial t} = -v \frac{\partial C_f}{\partial z} + \frac{D_m \phi_m}{b} \left\langle \frac{\partial C_p}{\partial x} \right\rangle_{x=b} \quad (6)$$

$$\frac{\partial C_p}{\partial t} = D_m \frac{\partial^2 C_p}{\partial x^2} - \lambda C_p \quad (7)$$

It is of interest to note that the transformed equations (6) and (7) are mathematically equivalent to equations describing tracer transport subject to a decay process (with the decay constant λ) occurring in the matrix block only. As will be demonstrated later, this feature is important for obtaining our analytical solutions based on the existing solutions describing tracer transport subject to radioactive decay in fractured rock, such as those derived by Tang et al. (1981) and Sudicky and Frind (1982).

Assuming the existence of equilibrium at $t = 0$ and considering a continuous injection case, we can have initial and boundary conditions for (6):

$$C_f(z, 0) = 0 \quad (8-1)$$

$$C_f(0, t) = C_0 \quad (8-2)$$

$$C_f(\infty, t) = 0 \quad (8-3)$$

The initial and boundary condition for the matrix equation (7) are

$$C_p(x, z, 0) = 0 \quad (9-1)$$

$$C_p(b, z, t) = C_f(z, t) \quad (9-2)$$

$$\frac{\partial C_p}{\partial x}(B, z, t) = 0 \quad (9-3)$$

where B is the half fracture spacing (Figure 2). The coupling of the matrix to the fracture is expressed by (9-2). Note that (9-3) is applied to multiple-fracture systems. For a single-fracture system, it may be replaced by (Tang et al., 1981)

$$C_p(\infty, z, t) = 0 \quad (9-4)$$

3. Analytical Solutions for a Single-Fracture System

We will start with deriving analytical solutions for a single-fracture system. Although a single-fracture system rarely exists in reality, it is a good approximation for many realistic fractured rocks when tracer penetration depth is much smaller than fracture spacing, because in this case, effects of surrounding fractures can be ignored. Analytical solutions are obtained with the strategy used by Tang et al. (1981) and Sudicky and Frind (1982) for developing analytical solutions to radioactive tracer transport in fractured rock. Specifically, we apply Laplace transformation to (7) and solve the transformed equation in Laplace space first, and then apply Laplace transformation to (6). The transformed equations are coupled through the term describing mass transfer between fractures and rock matrix and Equation (9-2). Finally, solutions in the Laplace space are inverted.

Applying Laplace transformation to (7) yields

$$pC_p' = D_m \frac{d^2 C_p'}{dx^2} - \lambda C_p' \quad (10)$$

where C_p' is the Laplace transformation of C_p and given by

$$C_p' = \int_0^{\infty} \exp(-pt) C_p(x, z, t) dt \quad (11)$$

Considering boundary conditions (9-2) and (9-4), the solution to ordinary differential equation (10) is obtained as

$$C_p' = C_f' \exp\{-EP^{1/2}(x-b)\} \quad (12)$$

where

$$E = D_m^{-1/2} \quad (13)$$

$$P = p + \lambda \quad (14)$$

and C_f' is the Laplace transformation of C_f . Based on (12), we have

$$\left\langle \frac{dC_p'}{dx} \right\rangle_{x=b} = -EP^{1/2} C_f' \quad (15)$$

Applying the Laplace transform to (6) yields

$$pC_f' + v \frac{dC_f'}{dz} = \frac{\phi_m D_m}{b} \left\langle \frac{dC_p'}{dx} \right\rangle_{x=b} \quad (16)$$

Substituting (15) into (16), we obtain the following solution to (16)

$$C_f' = \frac{C_0}{p} \exp\left(-\frac{pz}{v}\right) \exp\left(-\frac{P^{1/2}z}{vF}\right) \quad (17)$$

where

$$F = \frac{b}{\phi_m D_m^{1/2}} \quad (18)$$

The original tracer concentration C_f can be given in terms of the inverse transform L^{-1} as

$$C_f = L^{-1}(C_f') = \exp\left(\frac{\lambda z}{v}\right) L^{-1} \left[\exp\left(-\frac{\lambda z}{v}\right) C_f' \right] \quad (19)$$

Taking advantage of the fact that the inverse transform of $\exp\left(-\frac{\lambda z}{v}\right)C_f$, $C_r(z,t)$ was already reported by Tang et al. (1981) in their Equations (41) and (42). Thus, C_f can be directly obtained by multiplying $C_r(z,t)$ by $\exp\left(\frac{\lambda z}{v}\right)$ and the final result is

$$\frac{C_f}{C_0} = 0 \quad T < 0 \quad (20-1)$$

$$\frac{C_f}{C_0} = \frac{1}{2} \left[\exp\left(-\frac{\lambda^{1/2}z}{vF}\right) \operatorname{erfc}\left(\frac{z}{2vFT} - \lambda^{1/2}T\right) + \exp\left(\frac{\lambda^{1/2}z}{vF}\right) \operatorname{erfc}\left(\frac{z}{2vFT} + \lambda^{1/2}T\right) \right] \quad T > 0 \quad (20-2)$$

where

$$T = \left(t - \frac{z}{v}\right)^{1/2} \quad (20-3)$$

In some practical applications, it is often useful to relate tracer concentration signals to fracture surface areas, because the surface areas are important parameters for mass and heat transfer between mobile fluid in fractures and rock matrix. Under steady state flow conditions, we have the following conservation equation for fluid volume in fractures

$$Q\tau_f = Ab \quad (21)$$

where Q is fluid flux in a fracture (L^3/T), and A is the fracture surface area (L^2). In terms of fracture surface area, (20) can be rewritten as

$$\frac{C_f}{C_0} = 0 \quad T < 0 \quad (22-1)$$

$$\frac{C_f}{C_0} = \frac{1}{2} \left[\exp\left(-\frac{AD_m\phi_m}{LQ}\right) \operatorname{erfc}\left(\frac{AD_m^{1/2}\phi_m}{2QT} - \frac{D_m^{1/2}}{L}T\right) + \exp\left(\frac{AD_m\phi_m}{LQ}\right) \operatorname{erfc}\left(\frac{AD_m^{1/2}\phi_m}{2QT} + \frac{D_m^{1/2}}{L}T\right) \right] \quad T > 0 \quad (22-2)$$

where the diffusive reaction length defined by DePaolo (2006) as

$$L = \left(\frac{D_m}{\lambda}\right)^{1/2} \quad (22-3)$$

This reaction length (L) has the property that diffusion through the pore fluid is faster than reaction at length scales smaller than L , and reaction is faster than diffusion at length scales greater than L (DePaolo, 2006).

Using the properties of $\operatorname{erfc}(\infty) = 0$ and $\operatorname{erfc}(-\infty) = 2$, we can easily obtain the steady-state solution by taking the limit $T \rightarrow \infty$:

$$\frac{C_f}{C_0} = \exp\left(-\frac{\lambda^{1/2}z}{vF}\right) = \exp\left(-\frac{AD_m\phi_m}{LQ}\right) \quad (23)$$

4. Analytical Solutions for a Multiple-Fracture System

In the previous section, we derived analytical solutions for a single-fracture system which is a good approximation of many realistic fractured rocks when the tracer transport within fracture

does not significantly interact with tracer transport in surrounding fractures. However, for relatively small fracture spacing and/or long tracer travel times, interactions between adjacent fractures become important. In this case, solutions for multiple-fracture systems are needed for modeling tracer transport in fractured rock. Similar procedure for solving tracer transport problem in a single fracture system is followed here for a multiple-fracture system. Also note that governing equations are the same for both fracture systems except for some boundary conditions.

We first solve transformed tracer transport equation for rock matrix. The general solution to the transformed equation (10) is of the form (Sudicky and Frind, 1982)

$$C_p' = C_1 \cosh\{-EP^{1/2}(B-x)\} + C_2 \sinh\{-EP^{1/2}(B-x)\} \quad (24)$$

Based on boundary condition (9-3), we have $C_2 = 0$. Using boundary condition (9-2), we obtain C_1 and (24) becomes

$$C_p' = C_f' \frac{\cosh\{EP^{1/2}(B-x)\}}{\cosh\{\sigma P^{1/2}\}} \quad (25)$$

where again C_f' is the Laplace transformation of C_f and

$$\sigma = E(B-b) \quad (26)$$

The coupling between transformed tracer transport equations for fractures and matrix is done through the concentration gradient term in (16). In this case, that term is

$$\left\langle \frac{dC_p'}{dx} \right\rangle_{x=b} = -EP^{1/2}C_f' \tanh(\sigma P^{1/2}) \quad (27)$$

Then the transformed equation for tracer transport in fracture (Equation 16) becomes

$$pC_f' + v \frac{dC_f'}{dz} = -\frac{\phi_m D_m}{b} EP^{1/2} \tanh(\sigma P^{1/2}) C_f' \quad (28)$$

The solution to the above equation subject to boundary condition defined by (8-2) is

$$C_f' = \frac{C_0}{p} \exp\left(-\frac{Pz}{v}\right) \exp\left(-\omega P^{1/2} \tanh(\sigma P^{1/2})\right) \quad (29)$$

where

$$\omega = \frac{\phi_m D_m^{1/2} z}{bv} \quad (30)$$

The original tracer concentration C_f can be determined by the inverse transform of C_f' . The inverse transform of $C_f' \exp\left(-\frac{\lambda z}{v}\right)$ was already derived by Sudicky and Frind (1982). Thus, C_f can be easily determined as the inverse transform of Sudicky and Frind (1982) multiplied by $\exp\left(\frac{\lambda z}{v}\right)$:

$$\frac{C_f}{C_0} = 0 \quad T^0 < 0 \quad (31-1)$$

$$\frac{C_f}{C_0} = \frac{1}{\pi} \exp\left(\frac{2\lambda z}{v}\right) \int_0^\infty I d\varepsilon \quad T^0 > 0 \quad (31-2)$$

where

$$I = \frac{\varepsilon}{\lambda^2 + \varepsilon^4/4} \exp(\varepsilon_R^0) \left[\exp(-\lambda T^0) \left\{ \frac{\varepsilon^2}{2} \sin(\varepsilon_i^0) - \lambda \cos(\varepsilon_i^0) \right\} + \frac{\varepsilon^2}{2} \sin(\Omega^0) + \lambda \cos(\Omega^0) \right] \quad (31-3)$$

$$\varepsilon_R^0 = -\frac{\omega \varepsilon}{2} \left(\frac{\sinh(\sigma \varepsilon) - \sin(\sigma \varepsilon)}{\cosh(\sigma \varepsilon) + \cos(\sigma \varepsilon)} \right) \quad (31-4)$$

$$\varepsilon_i^0 = \frac{\varepsilon^2 T^0}{2} - \frac{\omega \varepsilon}{2} \left(\frac{\sinh(\sigma \varepsilon) + \sin(\sigma \varepsilon)}{\cosh(\sigma \varepsilon) + \cos(\sigma \varepsilon)} \right) \quad (31-5)$$

$$\Omega^0 = -\frac{\omega \varepsilon}{2} \left(\frac{\sinh(\sigma \varepsilon) + \sin(\sigma \varepsilon)}{\cosh(\sigma \varepsilon) + \cos(\sigma \varepsilon)} \right) \quad (31-6)$$

$$T^0 = t - \frac{z}{v} \quad (31-7)$$

Similar to the analytical solutions to the single-fracture system as discussed in the previous section, Equation (31) can also be written in terms of diffusive reaction length defined in (22-3), fracture surface area A and liquid flux Q . In this case, we have

$$\frac{C_f}{C_0} = 0 \quad T^0 < 0 \quad (32-1)$$

$$\frac{C_f}{C_0} = \frac{1}{\pi} \exp\left(\frac{2AD_m^2 b}{L^2 Q}\right) \int_0^\infty I d\varepsilon \quad T^0 > 0 \quad (32-2)$$

$$\omega = \frac{\varphi_m D^{1/2} A}{Q} \quad (32-3)$$

$$T^0 = t - \frac{Ab}{Q} \quad (32-4)$$

5. Illustrative Examples

Analytical solutions for a single-fracture system and a multiple-fracture system are presented in Sections 3 and 4. As previously indicated, our focus is on solutions to tracer transport in fractures, because tracer concentration data are often obtained from fractures in practical applications (Neretnieks, 2002; DePaolo, 2006). Analyses of these tracer data are generally used to understand flow and transport processes in fractured rock and to infer values of important parameters characterizing the relevant processes including fracture-matrix interaction.

As previously indicated, the current study is mainly motivated by a practical need to characterize a geothermal system in a natural or artificially created fractured reservoir using natural isotopic tracers with different transport properties. A key parameter for determining the economic feasibility of a geothermal system is the fracture-matrix interfacial areas. In this section, we use the newly developed analytical solutions to demonstrate how sensitive tracer transport processes are to fracture-rock properties. The sensitivity is crucial for successful determination of reservoir properties by

analyzing data for natural tracers. Note that parameter values used in this section are typical for a geothermal system in fractured rocks; it may not be the case for other flow and transport systems.

The parameter values used in our illustrative examples are within the ranges given in DePaolo (2006) for studying isotopic tracer transport in a number of typical geothermal systems

Table 1. Parameter values used in illustrative examples.

bulk reactivity R_m	1.E-5 yr ⁻¹
matrix diffusion coefficient D_m	0.1 m ² /yr
matrix porosity $\frac{C_f}{C_0}$	0.01
mass ratio of solid to liquid phase M	250
distribution coefficient K_d	35
advective time in fracture $\frac{z}{v}$	0.1 yr.
fracture aperture $2b$	1.E-3 m

(Table 1). In this study, we use these parameter values for the purpose of demonstrating the usefulness of the analytical solutions, rather than investigating tracer transport in a practical problem.

Figure 3 shows tracer breakthrough curves for a multiple-fracture system with half fracture spacing $B = 2.0$ and 0.5 m, respectively. The relative concentration in this figure and other figures is defined as $\frac{C_f}{C_0}$. For the comparison purpose, a breakthrough curve for a single fracture system is also presented. All these breakthrough curves are obtained using the parameter values given above. For $B = 2.0$ m, results from the single fracture system (with infinite fracture spacing) and the multiple-fracture system are essentially identical, indicating that for a relatively large fracture spacing, impact of surrounding fractures can be ignored, as expected. This also demonstrates the consistence of analytical solutions obtained for the two systems. For travel time less than one year, all the breakthrough curves remain essentially the same, because tracer penetration depth during this time period is much smaller than the given fracture spacing values, and therefore tracer

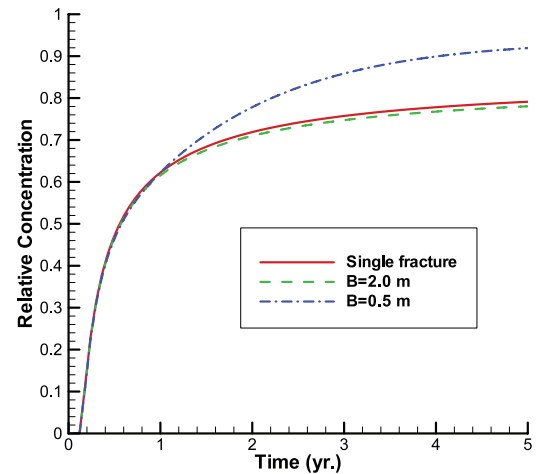


Figure 3. Breakthrough curves for a single fracture system and a multiple fracture system with half fracture spacing $B = 2.0$ and 0.5 m.

transport process is close to that for the single-fracture case. For a travel time longer than one year, tracer concentration for $B = 0.5$ m becomes larger than that for $B = 2.0$, resulting from that interaction between tracer transport from adjacent fractures reduces diffusive transport from fractures into matrix.

Figure 4 presents tracer breakthrough curves for a single-fracture system with two different L values (Equation 22-3). The base case corresponds to parameter values given at the beginning of this section and the other curve to the case with a L value reduced by half (or increased λ value that is 4 times as large as the base-case value). The two curves are very similar at an early time, but become considerably different later. The base case has a smaller λ value, and therefore a higher concentration at a later travel time. This example demonstrates the usefulness of viewing effects of precipitation-dissolution reactions as a “decay” process with decay constant λ that is proportional to the bulk reactivity in the matrix (Equation 5-3). The differences between the two

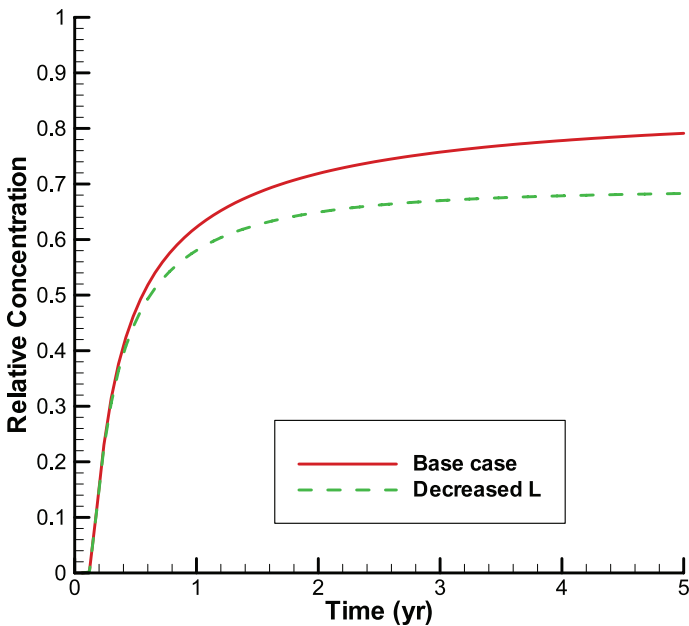


Figure 4. Breakthrough curves for a single fracture system with different L values. For the “Decreased L ” case, L is reduced by half from the value used in the base case.

curves in Figure 4 result from the fact that tracer mass loss owing to “decay” is time dependent and becomes significant only for a relatively long travel time.

Figure 5 shows breakthrough curves for a single fracture system with different values for matrix diffusion coefficient D_m . The base case and the “increased D_m ” case (dashed line) have the same parameter values (Table 1) except that the latter has a D_m value that is four times as large as the base case. As expected, a large diffusion coefficient gives relatively low concentration at a given time. This is because a larger matrix diffusion coefficient increases diffusive tracer transfer between a fracture and its surrounding matrix. An increased fracture-matrix surface area would play a similar role. Figure 5 also includes a third breakthrough curve that has the same (increased) D_m value as the dashed curve, but an increased λ value such that its L value is the same as the base case. Difference between the two “increased D_m ” cases is

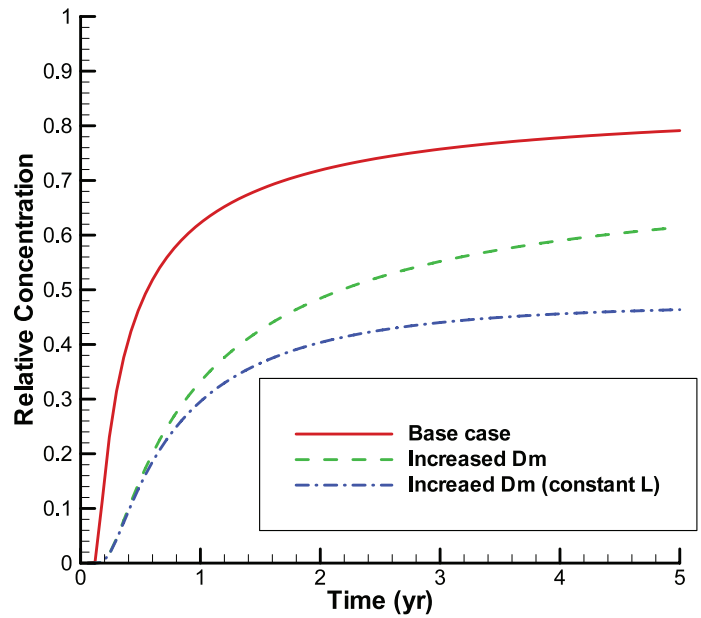


Figure 5. Breakthrough curves for a single fracture system with different D_m values. In the “Increased D_m ” case, the D_m value is four times as large as that in the base case.

similar to the difference between the two curves shown in Figure 4 as a result of effects of “decay” processes with different λ values.

In summary, the illustrative examples show that results are sensitive to rock and tracer properties for parameter values typical for a geothermal system (DePaolo, 2006), indicating that the relevant flow and transport parameters for a geothermal reservoir may be estimated by analyzing tracer signals. We also like to emphasize that our analytical solutions are developed based on several assumptions and approximations. One of them is that change in tracer concentration of the solid phase is not significant. The adequacy of this approximation for isotopic tracer transport

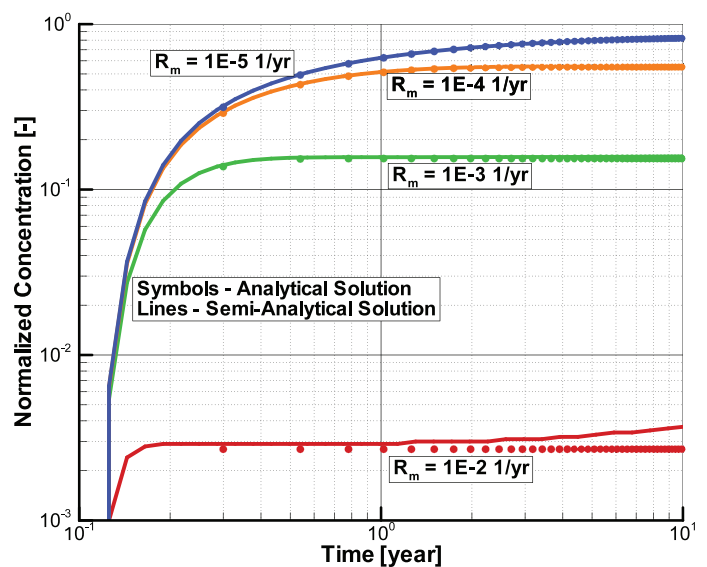


Figure 6. Comparisons between simulation results obtained from the current analytical solutions and semi-analytical solutions in Mukhopadhyay et al. (2010). Parameter values in Table 1 and $B = 0.5$ m are used for all the simulations except R_m .

was demonstrated in DePaolo (2006). Most recently, Mukhopadhyay et al. (2010) developed a semi-analytical solution that is not constrained by the constant c_s assumption. In that case, they were not able to obtain closed-form solutions, and instead numerically performed the inverse of Laplace transformations. As indicated in Figure 6, results from their solutions are identical to those obtained from our analytical solutions for small reaction rates that are typical for natural isotopic tracers, which is consistent with the finding of DePaolo (2006).

6. Conclusions

While significant progress has been made in developing analytical solutions for tracer transport in fractured rock under a variety of conditions, analytical solutions for tracer transport associated with precipitation-dissolution reactions are limited in the literature. These reactions are important for a number of applications such as characterizing an EGS system by interpreting tracer signals.

This study develops analytical solutions for tracer transport in both a single-fracture and a multiple-fracture system associated with precipitation-dissolution reactions under transient and steady state transport conditions. These solutions also take into account advective transport in fractures and molecular diffusion in rock matrix. It is demonstrated that for studying distributions of disturbed tracer concentration (defined as difference between actual concentration and its equilibrium value), effects of precipitation-dissolution reactions are mathematically equivalent to a “decay” process with a decay constant proportional to the corresponding bulk reaction rate. This important feature significantly simplifies our derivation procedure by taking advantage of the existence of analytical solutions to tracer transport associated with radioactive decay in fractured rock. It is also useful for interpreting tracer breakthrough curves, because the impact of decay processes is relatively easy to analyze. Several illustrative examples (breakthrough curves obtained from analytical solutions) are presented

and show that results are considerably sensitive to fracture spacing, matrix diffusion coefficient (fracture surface area), and bulk reaction rate (or “decay” constant), indicating that the relevant flow and transport parameters may be estimated by analyzing tracer signals.

Acknowledgement

The original version of the manuscript was reviewed by Drs. Dan Hawkes and Dmitriy Silin at LBNL. This work was supported by the American Recovery and Reinvestment Act (ARRA), through the Assistant Secretary for Energy Efficiency and Renewable Energy (EERE), Office of Technology Development, Geothermal Technologies Program, of the U.S. Department of Energy under Contract No. DE-AC02-05CH11231.

References

- DePaolo D.J., 2006. “Isotopic effects in fracture-dominated reactive fluid-rock systems.” *Geochimica et Cosmochimica Acta*, v. 70, p.1077-1096.
- Maloszewski P., and A. Zuber, 1985 “On the theory of tracer experiments in fissured rocks with a porous matrix.” *J Hydrology*, v. 79, p.333-358.
- MIT, 2007. “The future of geothermal energy.” Massachusetts Institute of Technology, MA.
- Mukhopadhyay S., H.H. Liu, N. Spycher and B. M. Kennedy, 2010. “Semi-analytical solutions for transient transport of a tracer in fractured rocks including fluid-rock interactions.” LBNL report, Lawrence Berkeley National Laboratory, Berkeley, CA.
- Neretnieks I., 2002. “A stochastic multi-channel model for solute transport – analysis of tracer tests in fractured rock.” *J Contaminant Hydrology*, v. 55, p.175-211.
- Sudicky E.A., and E.O. Frind, 1982. “Contaminant transport in fractured porous media: Analytical solutions for a system of parallel fractures.” *Water Resour Res*, v.18(6), p.1634-1642.
- Tang D.H., E.O. Frind, and E.A. Sudicky. 1981. “Contaminant transport in fractured porous media: Analytical solution for a single fracture.” *Water Resour Res* v.17, p. 555-564.

